Degradation behavior of electrical properties of GaInAs (1.0 eV) and GaInAs (0.7 eV) sub-cells of IMM4J solar cells under 1-MeV electron irradiation*

Yan-Qing Zhang(张延清)[1], Ming-Xue Huo(霍明学)[2], Yi-Yong Wu(吴宜勇)[1,2,†], Cheng-Yue Sun(孙承月)[2], Hui-Jie Zhao(赵慧杰)[1], Hong-Bin Geng(耿洪滨)[1], Shuai Wang(王帅)[3], Ru-Bin Liu(刘如彬)[3], and Qiang Sun(孙强)[3]

[1] *School of Materials Science & Engineering, Harbin Institute of Technology, Harbin* 150001, *China*
[2] *Research Center of Basic Space Science, Harbin Institute of Technology, Harbin* 150001, *China*
[3] *The* 18*th Research Institute of China Electronics Technology Group Corporation, Tianjin* 300381, *China*

(Received 4 March 2017; revised manuscript received 21 April 2017; published online 20 June 2017)

In this work the degradation effects of the $Ga_{0.7}In_{0.3}As$ (1.0 eV) and $Ga_{0.42}In_{0.58}As$ (0.7 eV) sub-cells for IMM4J solar cells are investigated after 1-MeV electron irradiation by using spectral response and photoluminescence (PL) signal amplitude analysis, as well as electrical property measurements. The results show that, compared with the electrical properties of traditional single junction (SJ) GaAs (1.41 eV) solar cell, the electrical properties (such as I_{sc}, V_{oc}, and P_{max}) of the newly sub-cells degrade similarly as a function of $\log\varphi$, where φ represents the electron fluence. It is found that the degradation of V_{oc} is much more than that of I_{sc} in the irradiated $Ga_{0.42}In_{0.58}As$ (0.7 eV) cells due to the additional intrinsic layer, leading to more serious damage to the space charge region. However, of the three types of SJ cells with the gap widths of 0.7, 1.0, and 1.4 eV, the electric properties of the $Ga_{0.7}In_{0.3}As$ (1.0 eV) cell decrease largest under each irradiation fluence. Analysis on the spectral response indicates that the J_{sc} of the $Ga_{0.7}In_{0.3}As$ (1.0 eV) cell also shows the most severe damage. The PL amplitude measurements qualitatively confirm that the degradation of the effective minority carrier life-time (τ_{eff}) in the SJ $Ga_{0.7}In_{0.3}As$ cells is more drastic than that of SJ GaAs cells during the irradiation. Thus, the output current of $Ga_{0.7}In_{0.3}As$ sub-cell should be controlled in the irradiated IMM4J cells.

Keywords: IMM4J, $Ga_{0.7}In_{0.3}As$ (1.0 eV), $Ga_{0.42}In_{0.58}As$ (0.7 eV), electrical properties

PACS: 88.40.jp, 88.40.H–, 88.40.fh **DOI:** 10.1088/1674-1056/26/8/088801

1. Introduction

In order to meet the requirements for the development of the space missions, progress in the performance of space solar cells has been remarkable, with device photoelectric conversion efficiency increasing by 0.5% each year for the past 50 years and more. Nowadays virtually every spacecraft is powered by high efficiency III–V three-junction (GaInP/GaAs/Ge) devices. But as these three-junction (3J) designs are approaching their efficiency limit, new four-junction (4J) designs are desired to drive efficiency higher. The 1.89/1.41/1.0/0.7-eV 4J inverted metamorphic multi-junction (IMM4J) solar cell targets an optimal band gap combination by utilizing the lattice-mismatched materials.[1,2] Hence, an IMM4J solar cell could be designed with two independently lattice-mismatched $Ga_xIn_{1-x}As$ junctions (the band-gaps of 1.0 eV and 0.7 eV at the compositions of $x = 0.7$ and 0.42) besides the traditional GaInP (1.89 eV) and GaAs (1.41 eV) sub-cells on the top. The IMM4J (GaInP/GaAs/$Ga_{0.7}In_{0.3}As$/$Ga_{0.42}In_{0.58}As$) has been reported to achieve efficiency over 40% under AM0 illumination over time.[3,4] However, lattices for the two lattice-mismatched sub cells ($Ga_{0.7}In_{0.3}As$ and $Ga_{0.42}In_{0.58}As$) have substantially 2.1% and 4.2% misfits to the GaAs substrate, respectively, imposing difficult in growing high-quality materials. Therefore, compositionally graded buffers (CGB) allow strain-free growth of the lattice-mismatched materials. During the growth of the buffer, the strain is relieved by the intentional formation and glide of dislocations.[5]

According to this principle, researchers at the National Renewable Energy Laboratory (NREL) introduced the IMM solar cell in 2005.[6] IMM3J solar cells with a band-gap arrangement of GaInP (1.89 eV)/GaAs (1.41 eV)/$Ga_{0.7}In_{0.3}As$ (1.0 eV) have achieved an efficiency of over 33% under 1 Sun AM0 or greater illumination, while the efficiency of conventional tri-junction (TJ) devices was limited to just around 30%.[7] Furthermore, the NREL team demonstrated a record conversion efficiency of 40.8% under 326 Suns (AM1.5G illumination).[8,9] By adding a fourth 0.7-eV sub-cell ($In_{0.58}Ga_{0.42}As$) to increase the bandwidth of the conversion spectrum, Emcore and Spectrolab developed an IMM4J device, which was characterized by a record conversion efficiency of 33.9% at 1-Sun AM0.[10–12]

With the technical efficiency of the IMM solar cells developing, more researchers are paying their attention to efficiency improvement. Solar cells are a major electric energy source for

*Project supported by the National Natural Science Foundation of China (Grant No. 11475049).
†Corresponding author. E-mail: wuyiyong@hit.edu.cn
© 2017 Chinese Physical Society and IOP Publishing Ltd

spacecraft, which inevitably experience the irradiation of energetic charged particles in orbit, leading to an obvious degradation in electric properties. It is of significance to investigate the irradiation effects of the charged particles on solar cells, in order to properly assess their performance in orbit and to improve the resistance to space irradiation.[13,14]

However, in spite of the fact that the IMM4J solar cell is the most important candidate for next generation space solar cells, the irradiation damage behaviors of the two different compositional lattice-mismatched sub-cells ($Ga_{0.7}In_{0.3}As$ and $Ga_{0.42}In_{0.58}As$) have not been adequately reported. As far as the authors know, Spectrolab just reported on the preliminary results of the power remaining factor after electron irradiation and put forward a possible theory, though they provided no systematic explanation of the damage mechanism.[5] Furthermore, a team from the University of Houston simulated the J_{sc} degradation behaviors of different sub-cells due to electron irradiation by modeling the irradiated defect tolerance, but obtained no further experimental results for verification.[15,16] The $Ga_{0.7}In_{0.3}As$ (1.0 eV) and $Ga_{0.42}In_{0.58}As$ (0.7 eV) sub-cells have different fabrication procedures and configurations compared with the sub-cells of conventional TJ device (GaInP/GaAs/Ge). For this reason, the ascertaining of the deterioration of their electrical properties (and derivation of their degradation model) has become a precondition of space application.

In this paper, 1-MeV electron irradiation tests are carried out on the $Ga_{0.7}In_{0.3}As$ (1.0 eV) and $Ga_{0.42}In_{0.58}As$ (0.7 eV) cells, and the degradation behaviors of their electrical properties are investigated. Finally, compared with the damage mechanism of GaAs (1.41 eV) sub-cells, through the analysis of the spectral response and the experimental PL experimental results, the damage mechanisms of the $Ga_{0.7}In_{0.3}As$ (1.0 eV) and $Ga_{0.42}In_{0.58}As$ (0.7 eV) cells are also qualitatively discussed.

2. Experiment

Samples of the specialized SJ $Ga_{0.7}In_{0.3}As$ (1.0 eV) and $Ga_{0.42}In_{0.58}As$ (0.7 eV) cells with a surface area of 2 cm×2 cm were supplied by the China Electronics Technology Group, Eighteenth Research Institute in Tianjin. Both kinds of SJ samples were epitaxially grown on lattice-mismatched GaAs substrate with using CGB technology by the metal–organic chemical vapor deposition (MOCVD) technique. Figure 1(a) shows the configuration schematics of the $Ga_{0.7}In_{0.3}As$ (1.0 eV) cell used in this study. Six step-graded buffer layers with a total thickness of 3000 nm are sandwiched between the GaAs growth substrate and $Ga_{0.7}In_{0.3}As$ (1.0 eV) cell. The base region was doped with 1×10^{17} cm^{-3} p-type doping, and the doping layer thickness was 2000 nm. The emitter region was doped with n^+-type doping in a concentration range of 1×10^{18} cm^{-3}, and the doping layer thickness was 300 nm. Figure 1(b) shows the configuration schematics of the $Ga_{0.42}In_{0.58}As$ (0.7 eV) cell, which is sequentially epitaxially grown on the n-type $Ga_{0.7}In_{0.3}As$ materials. The p-base doping concentration was 1×10^{17} cm^{-3}, and the doping layer thickness was 1700 nm. The n^+-emitter region doped with 2×10^{18} cm^{-3}, and the doping layer thickness was 300 nm. An intrinsic layer of $Ga_{0.42}In_{0.58}As$ (0.7 eV) is between the n^+–p junction with a thickness of 100 nm to offset the limit of V_{oc} due to the junction on both sides, lightly doped and heavily doped, to produce a smaller band bending the n^+–p junction.

The electron irradiation was performed at DD12-type Van der Graaf electron accelerators at the Heilongjiang Institute of Applied Physics. The samples were irradiated using 1-MeV electron beams with fluences of 1×10^{14}, 5×10^{14}, 8×10^{14}, 1×10^{15} cm^{-2} at room temperature. The irradiation flux was kept constant (1×10^{11} $cm^{-2}\cdot s^{-1}$).

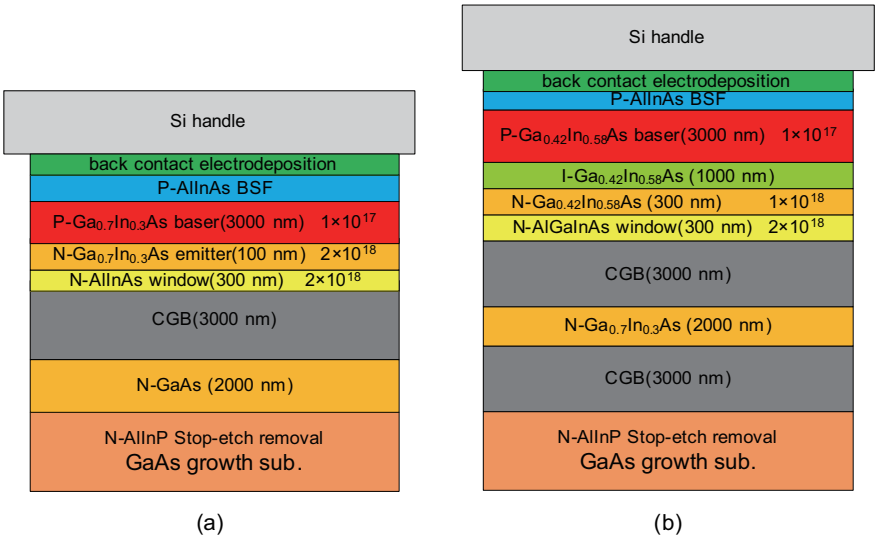


Fig. 1. (color online) Configurations of the sub-cells of (a) $Ga_{0.7}In_{0.3}As$ (1.0 eV) and (b) $Ga_{0.42}In_{0.58}As$ (0.7 eV). The grown structure is affixed to an Si handle and then the GaAs growth substrate is removed.

The electrical properties of the irradiated $Ga_{0.7}In_{0.3}As$ (1.0 eV) and $Ga_{0.42}In_{0.58}As$ (0.7 eV) solar cell before and after irradiation were measured under AM0 illumination using an HSC1 Solar Cell Tester from Shanghai Hi-Show PV Science & Technology Co., Ltd. Figures 2(a) and 2(b) show the *I–V* curves for the as-grown $Ga_{0.7}In_{0.3}As$ (1.0 eV) and $Ga_{0.42}In_{0.58}As$ (0.7 eV) cells, respectively. The short-circuit current (I_{sc}), open-circuit voltage (V_{oc}), and conversion efficiency of the as-grown $Ga_{0.42}In_{0.58}As$ (0.7 eV) cells were measured to be 133.0 mA, 0.289 V, and 4.99%, respectively and for the $Ga_{0.7}In_{0.3}As$ (1.0 eV) cells the data were 115.7 mA, 0.516 V, and 9.63% correspondingly. In this study, the spectral response spectra (SRS) curves in the wavelengths from 300 nm to 1700 nm were also measured using a solar cell quantum efficiency measurement system (model QEX10) from the PV Measurements Inc., USA.

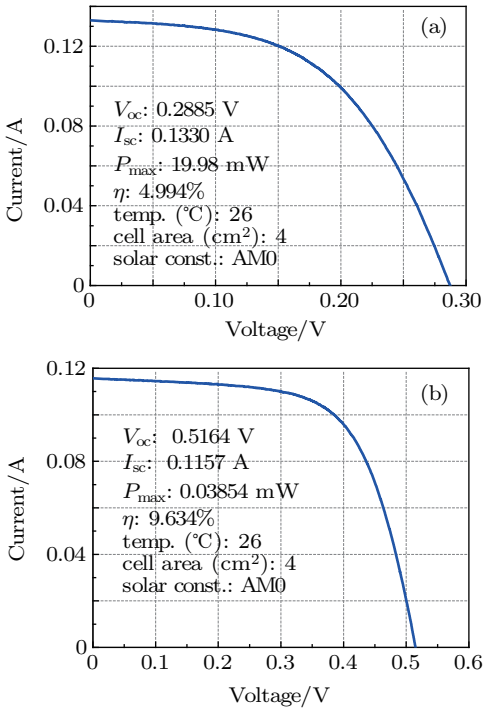


Fig. 2. (color online) *I–V* curves of the as-grown (a) $Ga_{0.42}In_{0.58}As$ (0.7 eV) and (b) $Ga_{0.7}In_{0.3}As$ (1.0 eV) cells.

In order to measure the photoluminescence (PL) signals and analyze the irradiated damage mechanisms on the subcells of the IMM4J solar cell, the SJ GaAs, which had a similar configuration and doping concentration was prepared using the same procedures as those seen in Fig. 3).

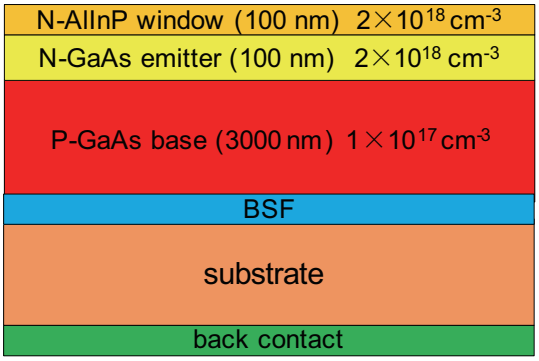


Fig. 3. (color online) Configuration of the GaAs (1.41 eV) cells.

The PL experimental system that was used is shown in Fig. 4.[17] The internally modulated 808 nm and 1064 nm diode lasers were employed as the excess carrier excitation sources of the SJ GaAs and $Ga_{0.7}In_{0.3}As$ cells, respectively. The laser beam was focused on the point on the solar cell surface, which was coincident with the focal point of an off-axis parabolic mirror that was used to collect a portion of the photons. The collected light was focused onto an InGaAs detector (Throlabs PDA10CS) with a switchable gain pre-amplifier (0 dB to 70 dB) and a frequency response of up to 17 MHz. The detector had a spectral bandwidth in a range from 800 nm to 1700 nm with a peak response 0.95 A/W at 1550 nm and an active element with an area of 0.79 mm^2. The long pass filter LP-1000 nm and LP-1150 nm were placed in front of the detector to detect the PL signals of the SJ GaAs and $Ga_{0.7}In_{0.3}As$ cells in order to block the excitation laser beam from the InGaAs detector. The PL measurements using the focused laser beam were carried out at room temperature; the output power densities of both lasers were continuously adjustable within a range from 0 mW/cm^2 to 600 mW/cm^2. Using the detected PL signals, the minority carrier life-time could be calculated, thus allowing us to determine the irradiation damage mechanisms.

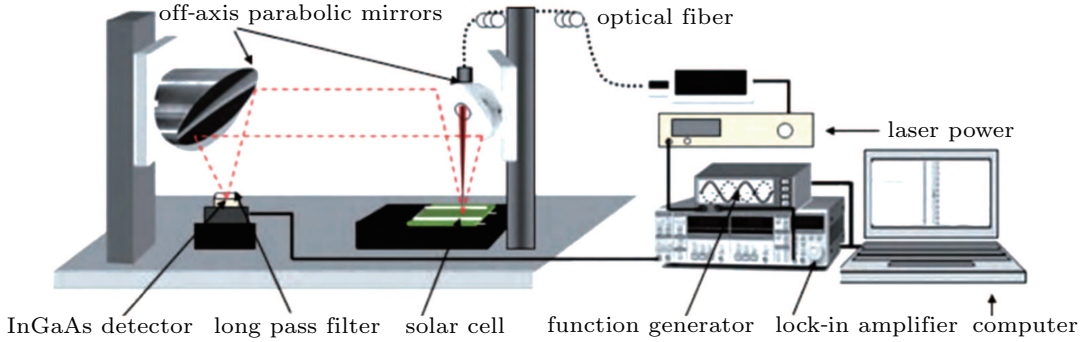


Fig. 4. (color online) Schematic diagram of the PL experimental system.

3. Results and discussion

3.1. Changes in electrical properties

Comparing with the as-grown electrical properties, figure 5 shows the remaining factors of I_{sc}, V_{oc}, and P_{max} of the $Ga_{0.7}In_{0.3}As$ (1.0 eV), $Ga_{0.42}In_{0.58}As$ (0.7 eV), and GaAs (1.41 eV) cells after being irradiated by 1-MeV electron beam. It has been shown that for the SJ GaAs solar cells, the electrical properties decrease gradually with the electron fluence increasing up to 1×10^{15} cm^{-2}. Furthermore, the experimental data (I_{sc}, V_{oc}, and P_{max}) could also be fitted as a function of $\log\varphi$ as follows:

$$\varphi P = 1 - c_p \log(1+\varphi/\varphi_{0p}), \tag{1}$$

where φ represents the electron fluence.[18,19] P represents the various electrical properties (I_{sc}, V_{oc}, and P_{max}), and the fitted parameter c_p represents the corresponding degradation rate. Here, φ_{0p} is thought as the critical damage fluence for the cells, which relates to the epitaxial material type used, the cell configuration, the doping concentration, or even the type of incident particles, etc. Thus, the fitted curves are also shown in Fig. 5, and the fitted constants c_p and φ_{0p} are listed in Table 1.

Hence, valid adaptations of the fitted curves with the experimental data imply that, comparing with the typical GaAs cell, lattice mismatch metamorphous configuration of the cells may not exert different effects on the output electrical properties after 1-MeV electron irradiation. Compared with I_{sc} and V_{oc}, P_{max} exhibits the largest decrease with the fluence. It can be explained by the fact that the P_{max} is proportional to the product of the current and voltage. Figure 5(a) shows that up to a fluence of 1×10^{15} cm^{-2}, the biggest drop is produced down to only remaining at 54% for the $Ga_{0.7}In_{0.3}As$ (1.0 eV) cells, and the $Ga_{0.42}In_{0.58}As$ (0.7 eV) cells shows slightly higher remaining factor of 61%, but the GaAs cell is the best with remaining factor of up to 84%. On the other hand, the fitted parameters also illustrate that the P_{max} degradation rate of the $Ga_{0.42}In_{0.58}As$ (0.7 eV) (shown as $c_{P_{max}}$) is much faster so that the fitted curve appears almost linear with respect to the electron fluence, and the P_{max} degradation rate of the $Ga_{0.7}In_{0.3}As$ (1.0 eV) presents the lowest but its critical fluence (shown as $\varphi_{P_{max}}$) is 20 times more than GaAs's.

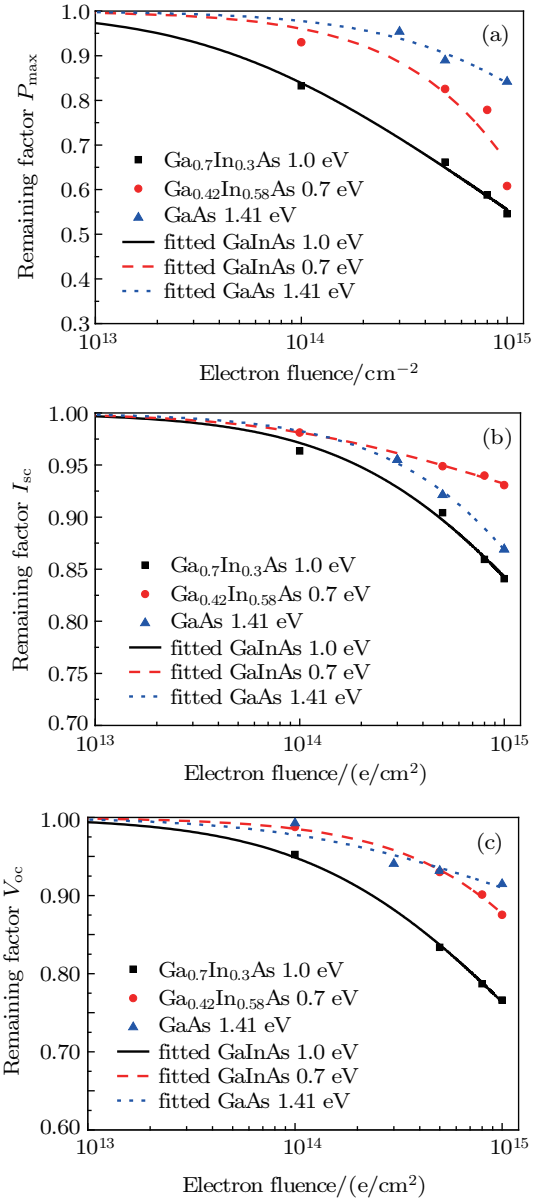


Fig. 5. (color online) Variations of remaining factors of (a) I_{sc}, (b) V_{oc}, and (c) P_{max} with fluence for $Ga_{0.42}In_{0.58}As$ (0.7 eV), $Ga_{0.7}In_{0.3}As$ (1.0 eV), and GaAs (1.41 eV) cells irradiated by 1-MeV electron.

Table 1. Fitted parameters of the degradation for V_{oc}, I_{sc}, and P_{max} in $Ga_{0.7}In_{0.3}As$ (1.0 eV), $Ga_{0.42}In_{0.58}As$ (0.7 eV), and GaAs cells after 1-MeV electron irradiation.

	I_{sc}		V_{oc}		P_{max}	
	$c_{I_{sc}}$	$\varphi_{I_{sc}}$	$c_{V_{oc}}$	$\varphi_{V_{oc}}$	$c_{P_{max}}$	$\varphi_{P_{max}}$
$Ga_{0.7}In_{0.3}As$	0.211	3.71×10^{14}	0.140	2.26×10^{14}	0.146	4.94×10^{14}
$Ga_{0.42}In_{0.58}As$	0.030	1.13×10^{14}	0.342	2.30×10^{15}	1	2.47×10^{15}
GaAs	0.144	6.46×10^{14}	0.045	1.55×10^{14}	0.228	9.69×10^{14}

Figures 5(b) and 5(c) show that both the I_{sc} and V_{oc} degradations of $Ga_{0.7}In_{0.3}As$ (1.0 eV) cells are the most significant, and the I_{sc} of $Ga_{0.42}In_{0.58}As$ (0.7 eV) cells decreases least; on the other hand the GaAs presents the lowest V_{oc} degradation. The I_{sc} degradation rate (shown as $c_{I_{sc}}$) of $Ga_{0.42}In_{0.58}As$ (0.7 eV) cells is 11.4 times slower than the degradation rate of V_{oc} (shown as $c_{V_{oc}}$), and the $c_{I_{sc}}$ of $Ga_{0.7}In_{0.3}As$ (1.0 eV) cells is almost the same as its $c_{V_{oc}}$. However, it is worth noting that the V_{oc} shows more significant degradation than the I_{sc} of the $Ga_{0.42}In_{0.58}As$ (0.7 eV) cells. This result is theoretically

inconsistent with the case of the conventional solar cells. For the single junction solar cells (such as Si and GaAs), the V_{oc} degradation rate should be slower than the I_{sc} as shown below.

$$V_{oc} = \frac{kT}{q} \log\left(\frac{I_{sc}}{I_0} + 1\right), \tag{2}$$

where I_0 is the saturation current, k is the Boltzmann constant, q is the electron charge, and T is the absolute temperature.[20,21] From the data in Table 1, it seems that the degradations of the I_{sc} and V_{oc} in $Ga_{0.7}In_{0.3}As$ (1.0 eV) cells follow this rule. But, in this study, the $c_{I_{sc}}$ and $c_{V_{oc}}$ of the $Ga_{0.42}In_{0.58}As$ (0.7 eV) are far more than the above theory. As is well known, the radiation-induced defects in the emitter and the base region can become the recombination centers of photo-generated carriers, making a portion of photo-generated carriers to be recombined before they have reached the junction region. This will cause the degradation in the I_{sc} of solar cells. On the other hand, the damage to the junction region mainly causes the V_{oc} to degrade. The recombination of carriers in the space-charge region can lead to an increase in the leakage current of diodes in the solar cell, and thus reducing the V_{oc}. In Fig. 1(a), there is a 0.1-μm intrinsic layer between the n^+–p junctions of the $Ga_{0.42}In_{0.58}As$ (0.7 eV). This design effectively improves the as-grown V_{oc}, but also greatly increases the space-charge region thickness. Thus more damages are deposited in the space-charge region by electron irradiation, which may become the reason for the V_{oc} of the $Ga_{0.42}In_{0.58}As$ (0.7 eV) to degenerate much faster than its I_{sc}.

3.2. Analysis of spectral response

Spectral response analysis is useful in evaluating the damage behavior of the SJ and multi-junction solar cells after charged particle irradiation.[18–20] The spectral response spectra are shown in Fig. 6 for the $Ga_{0.7}In_{0.3}As$ (1.0 eV) and $Ga_{0.42}In_{0.58}As$ (0.7 eV) solar cells after 1-MeV electron irradiation.

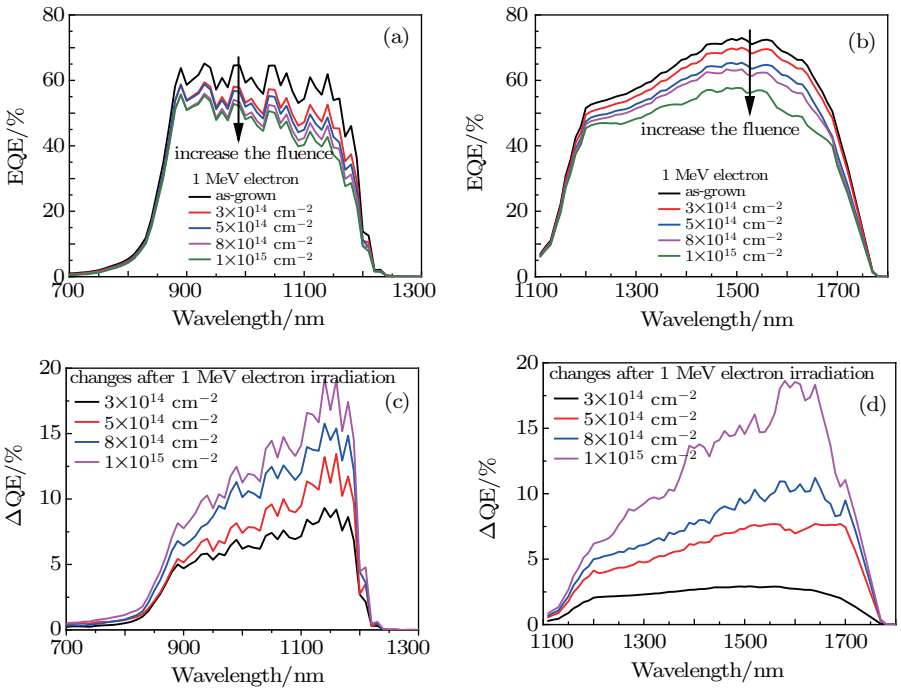


Fig. 6. (color online) Spectral response curves of (a) $Ga_{0.7}In_{0.3}As$ (1.0 eV) and (b) $Ga_{0.42}In_{0.58}As$ (0.7 eV) cells irradiated by 1-MeV electrons with various fluencies. The QE changes of the (c) $Ga_{0.7}In_{0.3}As$ (1.0 eV) and (d) $Ga_{0.42}In_{0.58}As$ (0.7 eV) cells.

Figure 6 shows that the spectral response spectra of both the $Ga_{0.7}In_{0.3}As$ (1.0 eV) and $Ga_{0.42}In_{0.58}As$ (0.7 eV) solar cells become degenerate with increasing the 1-MeV electron fluences, and the degradation profiles of the $Ga_{0.7}In_{0.3}As$ (1.0 eV) and $Ga_{0.42}In_{0.58}As$ (0.7 eV) cells are similar, namely more damages occur in the longer wavelength region. This phenomenon can be understood from the cell configuration and irradiation physics. The GEANT4 simulation indicates that 1-MeV electron irradiation could result in homogeneous damage to the $Ga_{0.7}In_{0.3}As$ (1.0 eV) and $Ga_{0.42}In_{0.58}As$ (0.7 eV) cells. This means that the irradiated defects should be distributed homogeneously in the active region of the cells. The defect quantity of the base region introduced by irradiation is more than that of the emitter region due to the difference in their thickness (the base region is 6.7 times thicker than the emitter region for the $Ga_{0.42}In_{0.58}As$ (0.7 eV) and nearly 5.7 times for the $Ga_{0.7}In_{0.3}As$ (1.0 eV)). The absorption coefficients (for both GaInP and GaAs) rise non-linearly with photo energy. This causes the light absorption thickness in the shorter wavelength region to be thinner than in the longer wavelength region. Hence, the photo-generated carriers produced by short-wavelength will result in a lower probability to

be trapped by the defect and more easily collected by the space charge region. Therefore, it can be concluded that more serious damage in the spectral response occurs within the long-wavelength region.

On the other hand, in order to quantify the degradation behaviors of $Ga_xIn_{1-x}As$ ternary compound solar cells irradiated by 1-MeV electrons, the values of short circuit current density (J_{sc}) of the $Ga_{0.7}In_{0.3}As$ (1.0 eV), $Ga_{0.42}In_{0.58}As$ (0.7 eV), and GaAs cells could also be measured using SRS tests. In order to keep the separated SJ cells consistent with the cases combined in IMM4J, the J_{sc} for the $Ga_{0.7}In_{0.3}As$ (1.0 eV) is integrated over the EQE data ranging only from 880 nm to 1240 nm, and the J_{sc} for the $Ga_{0.42}In_{0.58}As$ (0.7 eV) cells is integrated over a wavelength range from 1240 nm to 1800 nm. The corresponding J_{sc} remaining factors are presented in Fig. 7. Hence, it can be seen that the remaining factor of J_{sc} in the $Ga_{0.7}In_{0.3}As$ (1.0 eV) cell decreases more than that in the GaAs cell, while the $Ga_{0.42}In_{0.58}As$ (0.7 eV) cell shows the smallest damage. As electron fluence increases up to 1×10^{15} cm^{-2}, the J_{sc} of the $Ga_{0.7}In_{0.3}As$ (1.0 eV) cell decreases to 79.2% of the J_{sc} value in the as-grown case, while that of the GaAs cell decreases to 86.8% and the $Ga_{0.42}In_{0.58}As$ (0.7 eV) cell remains at 90.7%. These J_{sc} remaining factors could be fitted using Eq. (1) and the adaptive results are shown also in Fig. 7. Hence, the calculated constants of c and φ_0 are shown in Table 2. The maximum $c_{J_{sc}}$ appears in the $Ga_{0.7}In_{0.3}As$ (1.0 eV) cell compared with the other two, and its φ_0 value is slightly less than that of the GaAs cell but 3 times bigger than that of the $Ga_{0.42}In_{0.58}As$ (0.7 eV) cell. Moreover, the J_{sc} degradation of $Ga_{0.7}In_{0.3}As$ (1.0 eV) is consistent with the I_{sc} degradation (as seen in Fig. 5(b)). The result confirms that the $Ga_{0.7}In_{0.3}As$ (1.0 eV) cell presents the most serious damage after 1-MeV electron penetrable irradiation.

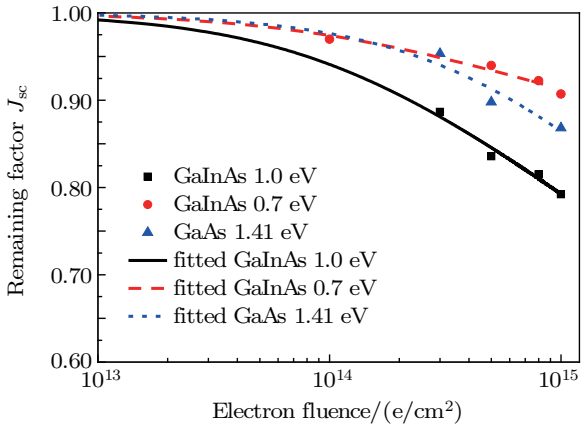


Fig. 7. (color online) Variations of remaining factor of J_{sc} with electron fluence for the $Ga_{0.7}In_{0.3}As$ (1.0 eV), $Ga_{0.42}In_{0.58}As$ (0.7 eV), and GaAs cells irradiated with 1-MeV electrons.

These results demonstrate that if the $Ga_{0.7}In_{0.3}As$ (1.0 eV), $Ga_{0.42}In_{0.58}As$ (0.7 eV), and GaAs cells are considered to be the three sub-cells of the IMM4J solar cell, the $Ga_{0.7}In_{0.3}As$ (1.0 eV) cell is confirmed to be the current-limit sub-cell for the irradiation resistance of the IMM4J solar cells. Meanwhile, it implies that the anti-irradiation capability of IMM cells can be enhanced by balancing the thickness of the $Ga_{0.7}In_{0.3}As$ (1.0 eV) sub-cell and adjusting the IMM cell configuration to obtain optimal current-limit for the three sub-cells.

Table 2. Fitted results of the J_{sc} of the $Ga_{0.7}In_{0.3}As$ (1.0 eV), $Ga_{0.42}In_{0.58}As$ (0.7 eV), and GaAs cells degradation after 1-MeV electron irradiation.

	$c_{J_{sc}}$	φ_0/cm^{-2}
$Ga_{0.7}In_{0.3}As$ (1.0 eV)	0.197	3.05×10^{14}
$Ga_{0.42}In_{0.58}As$ (0.7 eV)	0.036	0.93×10^{14}
GaAs (1.41 eV)	0.114	4.34×10^{14}

3.3. Effective life-time τ_{eff} from PL measurements

The decrease of the carrier life-time in irradiated solar cells is the primary reason for their electrical degradation. The PL analysis is one of the most valid methods used to evaluate the effective carrier life-time of solar cells. Hence, it is known that the PL signal I_{PL} and the rate of radiative recombination R_r are both proportional to the product of the electron and the hole carrier concentrations.[22] Accordingly, a relationship between the PL signal and the excess carrier life-time can be established. For a p-type base region solar cell with doping concentration N_A, a quadratic dependence on the excess carrier density $\Delta n$is expected from the PL signal I_{PL} to be as follows:

$$I_{PL} \propto R_r \approx B\Delta n(N_A + \Delta n), \tag{3}$$

where B is the radiative recombination coefficient.

The symmetry between a homogeneous emitter in the front side and a homogeneous back contact allows a one-dimensional (1D) excess carrier treatment of single junction solar cells. Under low injection condition, i.e., $\Delta n \ll N_A$, the depth-dependent carrier distribution in the base is described by the 1D steady-state version of differential Eq. (3):

$$\frac{d^2}{dz^2}\Delta n(z) - \frac{\Delta n(z)}{L^2} = \frac{-G(z)}{D_n}, \tag{4}$$

where L is the excess carrier diffusion length, G is the carrier generation rate, and D_n is the (minority) electron diffusion constant (in the p-type base region). In this case, assuming homogeneous carrier concentration within a sample at all times, the contributions of the excess carriers from the emitter can be neglected due to the high non-radiative recombination and the extreme shallowness (emitter thickness of around 100 nm compared with a base thickness of more than 3000 nm).[23] Correspondingly, the excess carrier distribution in the base usually plays a major role. The effective life-time τ_{eff} in the p-doped base of a solar cell under steady-state illumination condition is calculated from the carrier generation rate G and the

excess carrier density Δn. Equations (3) and (4) are simplified into

$$I_{\rm PL} \propto R_{\rm r} \approx B\Delta n N_{\rm A}, \tag{5}$$

$$\tau_{\rm eff} = \frac{\Delta n}{G}. \tag{6}$$

Here for the same solar cell G can be considered as a constant even after the electron irradiation is within the tested fluence.[24] Thus the PL signal change $\Delta I_{\rm PL}$ could be used to determine $\Delta\tau_{\rm eff}$ in SJ cells.

The amplitudes of the PL signals from the SJ GaAs and $Ga_{0.7}In_{0.3}As$ solar cell before and after the 1-MeV electron irradiation are illustrated in Fig. 8. From Figs. 8(a) and 8(b), it can be seen that with increasing electron fluence, the amplitudes of the PL signals of the irradiated GaAs and $Ga_{0.7}In_{0.3}As$ solar cells each present an approximate linear relationship with the excitation laser intensity. This indicates that with electron influence increasing up to 1×10^{15} cm^{-2}, the irradiation could not break the tested solar cells. However, it can also be seen that in both cases the PL signal amplitudes dramatically decrease. It implies that the irradiation induces a large number of defects in the solar cells, thus reducing the radiative recombination for PL emitting.

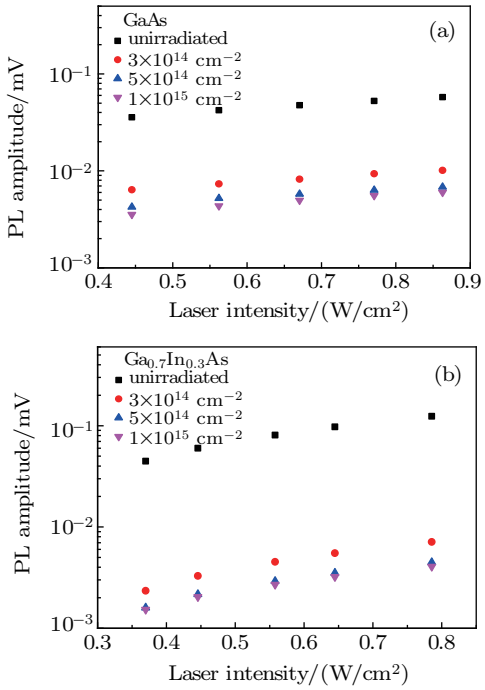


Fig. 8. (color online) Variations of amplitudes of PL signals with laser intensity of (a) GaAs and (b) $Ga_{0.7}In_{0.3}As$ cells obtained from experiment.

Irradiation induced defects would cause carrier life-time to decrease. According to the above-mentioned Eqs. (5) and (6), the degradation of the effective carrier life-time $\tau_{\rm eff}$ could be approximately equivalent to that of the PL signal. Figure 9 shows the dependence of normalized effective carrier life-time $\tau_{\rm eff}$ of GaAs and $Ga_{0.7}In_{0.3}As$ cells on electron fluence under different excitation laser intensities. It can be seen that in each of GaAs and $Ga_{0.7}In_{0.3}As$ cells, $\tau_{\rm eff}$ decreases drastically in the lower electron fluence till around 3×10^{14} cm^{-2}, then decreases slowly with increasing electron fluences. It should be noted that for GaAs and $Ga_{0.7}In_{0.3}As$ cells after 1×10^{15} cm^{-2} electron radiation,the values of effective life-time $\tau_{\rm eff}$ are calculated to be only 10% and 3% of the corresponding original ones, respectively. This indicates that the $Ga_{0.7}In_{0.3}As$ cell is more sensitive to irradiation damage than the GaAs one.

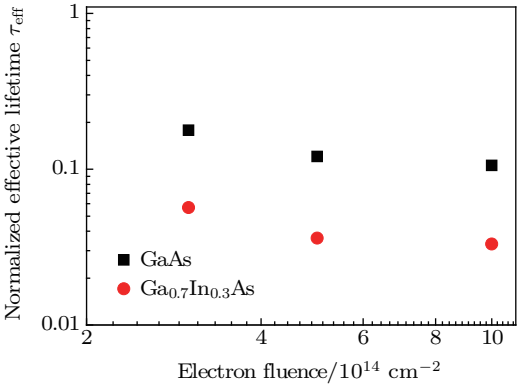


Fig. 9. (color online) Variations of normalized effective carrier life-time $\tau_{\rm eff}$ with irradiation electron fluence of GaAs and $Ga_{0.7}In_{0.3}As$ cells.

For a solar cell at a given photon flux Φ, the short circuit current $I_{\rm sc}$ can be given as follows:[25]

$$I_{\rm sc} = \Phi\left[1 - \frac{{\rm e}^{-\alpha W}}{1+\alpha\sqrt{L}}\right], \tag{7}$$

$$L = \sqrt{D_{\rm n}\tau_{\rm eff}}, \tag{8}$$

$$D_{\rm n} = \mu_{\rm n}(kT/q), \tag{9}$$

where α represents the absorption coefficient of the light, W is the width of the space charge region under zero bias, and $\mu_{\rm n}$ is the electron mobility.

From Eq. (7), with a given irradiation fluence, for different solar cells it holds true that the degradation of the $I_{\rm sc}$ is inversely proportional to minority carrier mobility μ and effective life-time $\tau_{\rm eff}$. It is understandable that the electron mobility keeps almost no change with irradiation (for $Ga_{0.7}In_{0.3}As$ and GaAs are 0.76×10^4 cm$^2\cdot$V$^{-1}\cdot$s^{-1} and 0.85×10^4 cm$^2\cdot$V$^{-1}\cdot$s^{-1}, respectively).[26] Thus a bigger decrement of the effective life-time $\tau_{\rm eff}$ in the $Ga_{0.7}In_{0.3}As$ solar cell would result in bigger $I_{\rm sc}$ degradation than in the GaAs cell. From the carrier transmission mechanism, these results of the degradation of $\tau_{\rm eff}$ would be reasonable to qualitatively explain why the $J_{\rm sc}$ of the $Ga_{0.7}In_{0.3}As$ sub-cell degrades more severely than that of GaAs sub-cell during the electron irradiation as shown in Fig. 7.

4. Conclusions

Our results demonstrate that 1-MeV electrons could lead to homogeneous damage to the $Ga_{0.7}In_{0.3}As$ (1.0 eV) and $Ga_{0.42}In_{0.58}As$ (0.7 eV) cells and the electrical properties degenerate as a function of $\log\varphi$ with irradiation fluence (φ).

Undoubtedly, of electric properties (P_{max}, V_{oc}, and I_{sc}), P_{max} exhibits the largest decrease due to the fact that it is proportional to the product of current and voltage. However, the V_{oc} degradation rate of the $Ga_{0.42}In_{0.58}As$ (0.7 eV) cells irradiated by 1-MeV electrons is much higher than the I_{sc} due to the additional intrinsic layer increasing the damage of the space charge region. Meanwhile, the electric properties of the $Ga_{0.7}In_{0.3}As$ (1.0 eV) cell all decrease greatly under each irradiation fluence condition. In addition, the degradation of V_{oc} is much higher than that of I_{sc} in the irradiated $Ga_{0.42}In_{0.58}As$ (0.7 eV) cells due to the additional intrinsic layer, leading to more serious damage to the space charge region. The SRS and PL amplitude analysis indicate that the bottom $Ga_{0.7}In_{0.3}As$ (1.0 eV) sub-cell shows the most severe damage during the 1-MeV electron irradiation. Accordingly, the PL amplitude measurements qualitatively verify that the τ_{eff} degradation of the irradiated $Ga_{0.7}In_{0.3}As$ sub-cell is more drastic than that of the GaAs sub-cell, causing the $Ga_{0.7}In_{0.3}As$ sub-cell to become the current-limit sub-cell in the IMM4J cells during the irradiation.

References

[1] Yamaguchi M, Takamoto T, Araki K and Ekins-Daukes N 2005 *Sol. Energy* **79** 78

[2] Friedman D J, Geisz J F, Norman A G and Wanlass M W 2006 *Conference Record of the* 2006 *IEEE* 4*th World Conference on Photovoltaic Energy Conversion*, May 7–12, 2006, Waikoloa, Hawaii, USA, 1 598

[3] Wilt D and Stan M 2012 *Industrial & Engineering Chemistry Research* **51** 11931

[4] France R M, Geisz J F, Steiner M A and Friedman D J 2013 *The* 38*th IEEE Photovoltaic Specialists Conference*, 2012, June 3–8, Austin, USA, 3 p. 893

[5] Patel P, Aiken D, Boca A and Cho B 2011 *The* 37*th IEEE Photovoltaic Specialists Conference*, 2011, June 19, Seattle, USA, 2 p. 377

[6] Wanlass M W, Ahrenkiel S P, Ahrenkiel R K and Albin D S 2005 *The* 31*th IEEE Photovoltaic Specialists Conference*, 2005, January 3–7, Springs, Coronado, USA, p. 530

[7] Rehder E M, Jun B, Chiu P and Wierman S 2014 *The* 39*th IEEE Photovoltaic Specialists Conference*, 2013, June 16–21, Tampa, Florida, USA, p. 3608

[8] Tatavarti R, Wibowo A, Martin G, Tuminello F, Youtsey C, Hillier G, Pan N, Wanlass M W and Romero M 2010 *The* 35*th IEEE Photovoltaic Specialists Conference*, 2010, June 20–25 Honolulu, Hawaii, USA, p. 2125

[9] Ma D Y, Chen N F, Fu R, Liu H, Bai Y M, Mi Z and Chen J K 2017 *Acta Phys. Sin.* **66** 048801 (in Chinese)

[10] Boisvert J, Law D, King R, Rehder E and Chiu P 2014 *The* 39*th IEEE Photovoltaic Specialists Conference*, 2013, June 16–21, Tampa, Florida, USA, 2 p. 2790

[11] Geisz J F, France R M, Steiner M A and Friedman D J 2014 *The* 10*th International Conference on Concentrator Photovaltics Systems*, 2014, April 7–9, Albuquerque NM, USA, 1616 p. 114

[12] Zhang X R, Li B C and Liu X M 2008 *Acta Phys. Sin.* **57** 7310 (in Chinese)

[13] Yue L, Wu Y Y, Zhang Y Q, Hu J M, Sun C Y, Hao M M and Lan M J 2014 *Acta Phys. Sin.* **63** 188101 (in Chinese)

[14] Gao X, Yang S S, Xue Y X, Li K and Li D M 2009 *Chin. Phys. B* **18** 5015

[15] Mehrotra A and Freundlich A 2013 *The International Society for Optical Engineering* (Proceedings of SPIE) **8620** 10030

[16] Razykov T M, Ferekides C S, Morel D, Stefanakos E, Ullal H S and Upadhyaya H M 2011 *Sol. Energy* **85** 1580

[17] Liu J Y, Song P, Wang F and Wang Y 2015 *Chin. Phys. B* **24** 097801

[18] Sato S, Miyamoto H, Imaizumi M, Shimazaki K and Morioka C 2009 *Sol. Energ. Mater. Sol. Cells* **93** 768

[19] Hu J M, Wu Y Y, Xiao J D, Yang D Z and Zhang Z W 2008 *Sol. Energ. Mater. Sol. Cells* **92** 1652

[20] Loo R Y, Kamath G S and Li S S 1990 *IEEE Trans. Electron Dev.* **37** 485

[21] Patel P, Aiken D, Chumney D and Cornfeld A 2012 *The* 38*th IEEE Photovoltaic Specialists Conference*, 2012, June 3–8, Austin, USA, 2 1

[22] Herlufsen S, Schmidt J, Hinken D, Bothe K and Brendel R 2008 *Rapid Research Letters* **2** 245

[23] Trupke T, Bardos R A and Abbott M D 2005 *Appl. Phys. Lett.* **87** 184102

[24] Synopsys Inc., Sentaurus Device, Synopsys Inc.

[25] Angelis N D, Bourgoin J C, Takamoto T, Khan A and Yamaguchi M 2001 *Sol. Energy Mater. Sol. Cells* **66** 495

[26] Levinshteim M, Rumyantsev S and Shur M 1996 *Handbook Series on Semiconductor Parameters*, Vol. 2 (Hong Kong: World Scientific) p. 78